Sn-*n*-$Bu_3(C_5Me_5)$, 69382-50-9; $\{Os(\eta^4\text{-}C_8H_{12})Cl_2\}_x$, 39395-16-9; HC_5Me_5, 4045-44-7; $Na_2[OsCl_6]$, 1307-81-9; $(\eta^5\text{-}C_5H_5)Ru(\eta^4\text{-}C_8H_{12})Cl$, 97913-63-8; $K[C_5H_4Me]$, 41066-45-9; $K[C_5Me_5]$, 94348-92-2.

Supplementary Material Available: Available: Listings of observed and calculated structure factors for decamethylruthenocene and decamethylosmocene (19 pages). Ordering information is given on any current masthead page.

Dynamics of Internal Motion in Nonacarbonyl(η^6-mesitylene)tetracobalt and Nonacarbonyl(η^6-triptycene)tetracobalt. Carbonyl Scrambling and Rotation about the Triptycene–Cobalt Axis

Roman A. Gancarz,[1a,b] Mary W. Baum,[1a] Geoffrey Hunter,[1c] and Kurt Mislow*[1a]

Departments of Chemistry, Princeton University, Princeton, New Jersey 08544, and The University, Dundee DD1 4HN, Scotland

Received January 30, 1986

Variable-temperature ^{13}C NMR studies of noncarbonyl(η^6-triptycene)tetracobalt (**1**) and nonacarbonyl(η^6-mesitylene)tetracobalt (**2**) are reported. The rate constants of carbonyl group exchange between bridging, equatorial, and axial sites have been determined from a line-shape analysis of the spectra, and it is found that the relative rates of the bridging–equatorial, bridging–axial, and axial–equatorial transposition processes in both compounds are markedly temperature-dependent. The plots of ln k vs. $1/T$ of both compounds show crossover regions in which the $\Delta G^{\ddagger}$ values of the three processes are almost the same: 10.8 kcal mol^{-1} at 225 K for **1** and 13.3 kcal mol^{-1} at 285 K for **2**. Rotation about the triptycene–cobalt axis in **1** is faster than carbonyl scrambling over the temperature range examined, 178–308 K. The activation energy for rotation is E_a = 8.2 kcal mol^{-1}.

The molecular structure of nonacarbonyl(η^6-triptycene)tetracobalt (**1**) shows clear evidence of strong repulsive interactions between the $Co_4(CO)_9$ fragment and the proximal ring of the triptycene moiety.[2] The same interactions are expected to manifest themselves in a substantial barrier to rotation about the arene–metal axis: although such barriers are generally quite low,[3] bulky substituents have the effect of increasing the activation energy.[4,5] In the case of **1**, this internal motion is accompanied by the scrambling of terminal and bridging carbonyl groups on the three basal cobalt atoms. In this paper we report the results of a variable-temperature NMR study whose aim was to obtain a quantitative measure of the energy barriers for all of these processes.

Results and Discussion

As a first step, we investigated the kinetics of carbonyl scrambling in nonacarbonyl(η^6-mesitylene)tetracobalt (**2**),[6] a π complex related to **1** in which rotation about the arene–cobalt axis is NMR-invisible because of molecular C_3 or C_{3v} symmetry (Figure 1).[7] The 62.83-MHz ^{13}C NMR

(1) (a) Princeton University. (b) On leave of absence from the Technical University, Wrocław, Poland. (c) University of Dundee.

(2) Gancarz, R. A.; Blount, J. F.; Mislow, K. *Organometallics* **1985**, *4*, 2028.

(3) Albright, T. A.; Hofmann, P.; Hoffmann, R. *J. Am. Chem. Soc.* **1977**, *99*, 7546 and references therein. Marder, T. B.; Baker, R. T.; Long, J. A.; Doi, J. A.; Hawthorne, M. F. *Ibid.* **1981**, *103*, 2988 and references therein.

(4) Pomeroy, R. K.; Harrison, D. J. *J. Chem. Soc., Chem. Commun.* **1980**, 661. Luke, W. D.; Streitwieser, A., Jr. *J. Am. Chem. Soc.* **1981**, *103*, 3241. Werner, H.; Hofmann, W. *Chem. Ber.* **1981**, *114*, 2681.

(5) Evidence for restricted rotation about the arene–chromium axis in dicarbonyl(η^6-hexaethylbenzene)thiocarbonylchromium is inconclusive. See: Hunter, G.; Mislow, K.; Weakley, T. J. R.; Wong, M. G. *J. Chem. Soc., Dalton Trans.* **1986**, 577 and references therein.

(6) (a) Bor, G.; Sbrignadello, G.; Marcati, F. *J. Organomet. Chem.* **1972**, *46*, 357. (b) Khand, I. U.; Knox, G. R.; Pauson, P. L.; Watts, W. E. *J. Chem. Soc., Perkin Trans. 1* **1973**, 975.

(7) By analogy with nonacarbonyl(η^6-benzene)tetracobalt, which has crystallographic C_3 symmetry,[8] and $Co_4(CO)_{12}$, whose ^{59}Co,[9] ^{13}C,[9] and ^{17}O[10] NMR spectra are all consistent with C_{3v} symmetry in solution.[11]

(8) Bird, P. H.; Fraser, A. R. *J. Organomet. Chem.* **1974**, *73*, 103.

(9) Aime, S.; Gobetto, R.; Osella, D.; Milone, L.; Hawkes, G. E.; Randall, E. W. *J. Magn. Reson.* **1985**, *65*, 308.

(10) Aime, S.; Osella, D.; Milone, L.; Hawkes, G. E.; Randall, E. W. *J. Am. Chem. Soc.* **1981**, *103*, 5920.

0276-7333/86/2305-2327$01.50/0

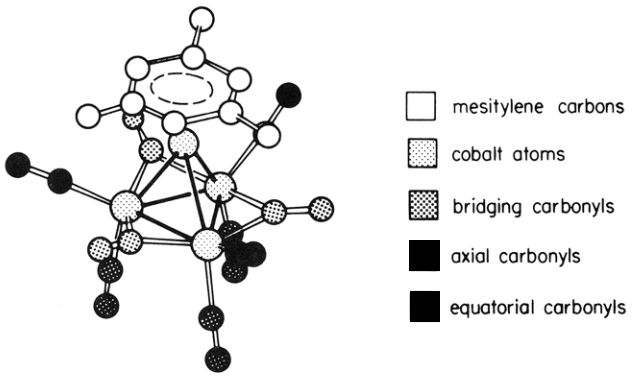

Figure 1. A possible C_3 conformation of nonacarbonyl(η^6-mesitylene)tetracobalt (**2**), modeled on the molecular structure of nonacarbonyl(η^6-benzene)tetracobalt.[8] Hydrogen atoms are not shown.

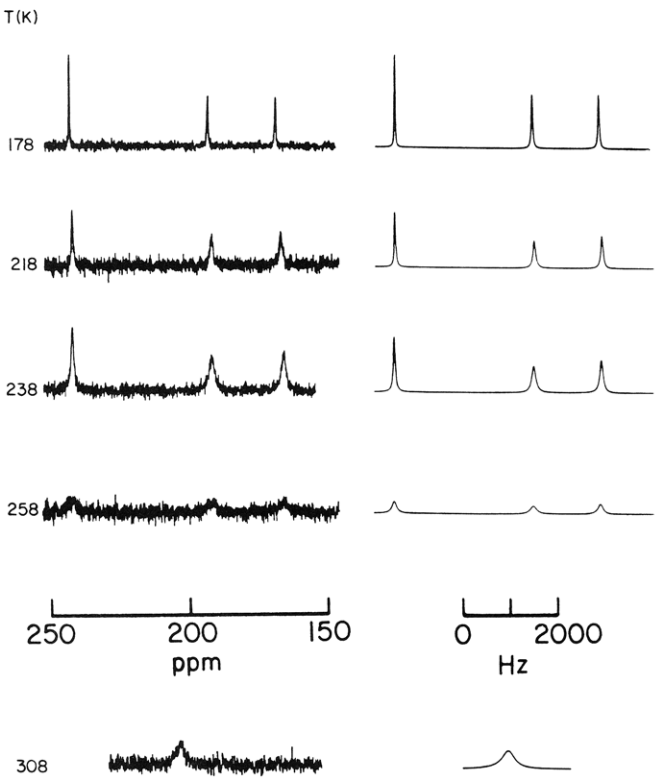

Figure 2. Left: selected variable-temperature ^{13}C NMR spectra (carbonyl region) of nonacarbonyl(η^6-mesitylene)tetracobalt (**2**) in CD_2Cl_2. Spectra at 258 K and below were measured at 62.83 MHz. The broad singlet at 308 K (δ 208.5 ($w_{1/2}$ = 220 Hz)) was measured at 22.50 MHz. Right: simulated spectra, using rate constants in Table I.

spectrum of **2** in CD_2Cl_2 at 178 K exhibits three singlets in the carbonyl region, δ 247.23 (ν_1), 197.25 (ν_2), and 172.68 (ν_3). By analogy with the corresponding η^6-toluene π complex,[12] the most downfield signal (ν_1) was assigned to the bridging carbonyl carbons, and by analogy to the assignment of chemical shifts in **1** (see below), ν_2 and ν_3 were assigned to the axial and equatorial carbonyl carbons, respectively.

Table I. Rate Constants for Carbonyl Group Transpositions in Nonacarbonyl(η^6-mesitylene)tetracobalt (2)

	temperature[b]						
rate const[a]	178	188	198	218	238	258	308
k_{13}	0.10	0.30	0.80	5.0	20	100	5000
k_{12}	2.0	11.5	20.5	45	83	220	1400
k_{23}	53	60	80	125	200	280	550

[a] k_{ij} (in s^{-1}) refers to the exchange between two sites i and j characterized by ^{13}C NMR resonances ν_i and ν_j. [b] In degrees Kelvin.

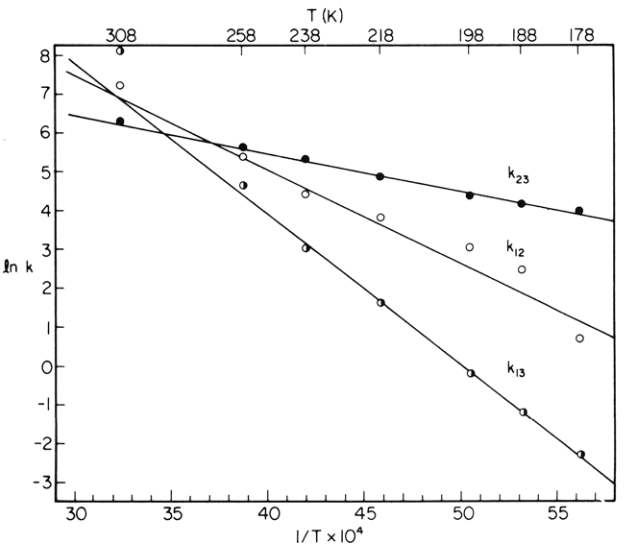

Figure 3. Arrhenius plots for the three carbonyl group transpositions (k_{ij}) in nonacarbonyl(η^6-mesitylene)tetracobalt (**2**).

At higher temperatures, the ^{13}C NMR signals broaden and eventually coalesce (Figure 2), indicative of carbonyl scrambling. That the process responsible for the observed site exchange is intramolecular was shown by a comparison of the mass spectrum of a mixture of ^{13}C-labeled and unlabeled **2** with the mass spectrum of the same mixture recovered from solution in CD_2Cl_2. It remained to determine whether more than one site-exchange process is responsible for the variation in line shape with temperature.

Among the rationalizations of fluxional behavior in related transition metal cluster carbonyls,[14] the classic example is the exchange mechanism in $Co_4(CO)_{12}$ via a T_d intermediate.[15] A single process is rate determining in this site exchange, as shown by a line-shape analysis of the variable-temperature ^{17}O NMR spectrum[10] in which all six rate constants in the four-site-exchange system were set to be equal.[16,17] In contrast, simulation of the variable-temperature NMR spectra of **2** required no fewer than three different rate constants, k_{12}, k_{13}, and k_{23}, to describe

(11) The molecular structure of $Co_4(CO)_{12}$ in the crystal also has approximate C_{3v} symmetry. See: Corradini, P. *J. Chem. Phys.* **1959**, *31*, 1676. Wei, C. H. *Inorg. Chem.* **1969**, *8*, 2384. Carré, F. H.; Cotton, F. A.; Frenz, B. A. *Ibid.* **1976**, *15*, 380. Also see ref 2.

(12) At 203 K, the ^{13}C NMR spectrum of nonacarbonyl(η^6-toluene)-tetracobalt in CD_2Cl_2 features three singlets of equal intensity at δ 247.3 (bridging carbonyl), 198.7 (terminal carbonyl), and 180.9 (terminal carbonyl).[13] The absence of resonance doubling down to 173 K[13] could be construed as evidence for unrestricted rotation about the arene–cobalt axis; alternatively, rotation might be slow at 173 K, but the small perturbation by the methyl group might not be sufficient to break the accidental signal isochrony.

(13) Evans, J.; Johnson, B. F. G.; Lewis, J.; Matheson, T. W.; Norton, J. R. *J. Chem. Soc., Dalton Trans.*, **1978**, 626.

(14) Johnson, B. F. G.; Benfield, R. E. *J. Chem. Soc., Dalton Trans.* **1978**, 1554 and references therein. Also see: Heaton, B. T.; Pergola, R. D.; Strona, L.; Smith, D. O. *Ibid.* **1982**, 2553. Band, E.; Muetterties, E. L. *Chem. Rev.* **1978**, *78*, 639, especially p 653 ff.

(15) Cotton, F. A. *Inorg. Chem.* **1966**, *5*, 1083.

(16) We simulated (program DNMR3[17]) the line shapes at +85, +57, +21, and −25 °C in ref 10 by using rate constants of 4000, 1200, 200, and 10 s^{-1}, respectively. Calculated Arrhenius parameters were E_a = 9.6 kcal mol^{-1} and ln A = 21.7 (ρ = 0.9999). No attempt was made to simulate the spectrum at −55 °C, where line broading is reportedly[10] due to the increased quadrupole relaxation of ^{17}O.

(17) Kleier, D. A.; Binsch, G. *QCPE* **1970**, *11*, 165.

Table II. Activation Parameters for Carbonyl Group Transpositions ($i \leftrightarrow j$) in Nonacarbonyl(η^6-mesitylene)tetracobalt (2)

parameter	process[a] 1 ↔ 3	1 ↔ 2	2 ↔ 3
E_a[b]	7.8	4.7	2.0
ln A	19.6	14.7	9.4
ρ[c]	0.9990	0.9652	0.9928

[a] $i \leftrightarrow j$ refers to the exchange between two sites characterized by ^{13}C NMR resonances ν_i and ν_j. [b] In kcal mol^{-1}. [c] Correlation coefficient for the least-squares line through the six k_{ij}'s in the temperature range 178–258 K (Table I).

Table III. Chemical Shift Assignments of Resonances in the Carbonyl Region of the ^{13}C NMR Spectrum of Nonacarbonyl(η^6-triptycene)tetracobalt in CD_2Cl_2 at 168 K

signal label	δ[a]	relative peak height[b]	carbonyl group label[c]	carbonyl group type
1A	251.10	18.5	6/9	bridging
1B	238.90	6.8	3	bridging
2A	196.48	25.0	1/4	axial
2B	196.48	25.0	7	axial
3A	174.28	14.5	2/5	equatorial
3B	169.67	6.4	8	equatorial

[a] The five signals listed here do not differ significantly in appearance from those depicted in the spectrum at 178 K (Figure 5). [b] In arbitrary units. Since there is some variation in line widths, relative peak heights are only an approximate measure of relative integrated intensities. [c] Atom labels refer to Figure 4.

exchanges between the three different carbonyl groups with resonances at ν_1, ν_2, and ν_3.[18] The results of the line-shape analysis are presented in Table I and in Figure 2.[19]

A glance at the data in Table I reveals the importance of entropic factors: process 1 ↔ 3, which is slowest at low temperatures, and process 2 ↔ 3, which is fastest at low temperatures, reverse roles at high temperatures. The three crossover points fall within the temperature range 270–310 K, as seen by inspection of the three Arrhenius plots (Figure 3). These plots were constructed by a least-squares fit of the set of six data points for each of the three processes in the range 178–258 K (Table I), corresponding to measurements at high field (62.83 MHz). Extrapolation to 308 K, corresponding to a measurement at low field (22.50 MHz),[21] yields values for k_{23} and k_{12} of 500 and 1040 s^{-1}, in fair agreement with the values of 550 and 1400 s^{-1} used in the line-shape analysis (Table I, Figure 2). However, the value of 1010 s^{-1} at 308 K calculated for k_{13} by the Arrhenius equation deviates significantly from the value of 5000 s^{-1} used in the line-shape analysis.

Table IV. Carbonyl Site-Exchange Processes at the Slow-Rotation Limit in Nonacarbonyl(η^6-triptycene)tetracobalt (1)

process[a]	type of carbonyl group undergoing site exchange and corresponding atom labels[b]	
	Bridging ↔ Equatorial	
1B ↔ 3A	3	2/5
1A ↔ 3A	6/9	2/5
1A ↔ 3B	6/9	8
1B ↔ 3B*	3	8
	Bridging ↔ Axial	
1B ↔ 2A	3	1/4
1A ↔ 2A	6/9	1/4
1A ↔ 2B	6/9	7
1B ↔ 2B*	3	7
	Axial ↔ Equatorial	
2A ↔ 3A	1/4	2/5
2B ↔ 3B	7	8
2A ↔ 3B*	1/4	8
2B ↔ 3A*	7	2/5

[a] Signal labels are identified in Table III. The asterisk designates a disallowed process (see text). [b] Atom labels refer to Figure 4.

Whether this indicates a change in mechanism at higher temperatures or merely reflects the difficulty of obtaining a unique solution[19] is impossible to say on the basis of the available information.

Arrhenius activation parameters are collected in Table II. Although activation parameters obtained by the complete line-shape method are often subject to serious errors,[22,23] we believe that the results of the present study are sufficiently reliable to warrant confidence in our main conclusion, that transpositions of carbonyl groups in **2** between magnetically nonequivalent sites (bridging ↔ axial, bridging ↔ equatorial, and axial ↔ equatorial) occur at distinguishable rates. Thus, at 285 K, near the middle of the crossover region (Figure 3), $\Delta G^\ddagger$ is 13.4, 13.1, and 13.3 kcal mol^{-1} for 1 ↔ 3, 1 ↔ 2, and 2 ↔ 3, respectively;

(18) We assume that ligand permutations are restricted to the nine carbonyl groups attached to the three basal cobalt atoms, while the arene ring remains attached to the apical cobalt atom in the conventional η^6-mode. However, the possibility cannot be strictly excluded that ligand scrambling on the Co_4 frame involves an unstable intermediate in which the arene ring is bonded to three cobalt atoms in a μ_3-η^2:η^2:η^2 face-capping mode. See: Gomez-Sal, M. P.; Johnson, B. F. G.; Lewis, J.; Raithby, P. R.; Wright, A. H. *J. Chem. Soc., Chem. Commun.* **1985**, 1682.

(19) A unique combination of two or more rate constants is difficult to obtain by line-shape analysis if the spectral shape is simple,[20] and up to 30 simulations were therefore performed with different sets of k's in order to obtain the best fits. Values of rate constants were chosen by trial and error, and the linearity of the Arrhenius plot was taken as a criterion for the correct choice of k's. Given the complexity of the analysis, it is virtually impossible to provide a meaningful estimate of the uncertainty in the values of the calculated rate constants and activation parameters, which are therefore reported without the customary error limits.

(20) Ōki, M.; Kono, M.; Kihara, H.; Nakamura, N. *Bull. Chem. Soc. Jpn.* **1979**, *52*, 1686.

(21) Because of the magnitude of the $\Delta\nu$ values, observation of a coalesced singlet at high fields requires inconveniently high temperatures.

(22) For example, see: Binsch, G.; Kessler, H. *Angew. Chem., Int. Ed. Engl.* **1980**, *19*, 411. Sandström, J. *Dynamic NMR Spectroscopy*; Academic Press: New York, 1982.

(23) The possibility exists that the observed line broadening is the result of ^{59}Co quadrupole relaxation. However, we believe that this is unlikely for the folowing reasons. First, the carbonyl groups in **1** and **2** are all attached to basal cobalt atoms, and line-width anomalies should be restricted to carbonyl carbons attached to the apical cobalt.[9,24a] Second, the 62.83- and 22.50-MHz spectra of **2** recorded at 308 K are markedly different: while a single broad signal is observed at 22.50 MHz, the broadening at 62.83 MHz is so extensive that the signal can barely be distinguished from the noise level. This clearly indicates that the broadening at higher temperatures is caused by exchange and not by quadrupole relaxation, which is field-independent.[24b] Unfortunately, it was not possible to observe the expected line narrowing at higher temperatures, due to the extensive decomposition of the complex at temperatures above 313 K. Note also that for **2**, the lines are sharp at the slow-exchange limit ($w_{1/2}$ = 20–30 Hz at 178 K) and not very broad even at the onset of exchange (the line width at half-height, $w_{1/2}$, is no more than 78 Hz at 218 K). Additionally, although at low temperatures ^{59}Co–^{13}C coupling is usually small due to rapid quadrupole relaxation, line broadening from this coupling might be expected to become more significant at higher temperatures as such relaxation becomes less efficient. However, the coalesced line simulated from the rate constants obtained by extrapolation using the Arrhenius equation is actually somewhat broader than that observed at 308 K, indicating that ^{59}Co coupling does not significantly contribute to the line broadening over the temperature range investigated. Finally, the intensities of the lines in the ^{13}C NMR spectrum of **2** are also independent of pulse delay time under conditions of exchange (218 K).

(24) (a) Darensbourg, D. J.; Zalewski, D. J. *Organometallics* **1985**, *4*, 92. (b) Becker, E. D. *High Resolution NMR Theory and Chemical Applications*; Academic Press: New York, 1980.

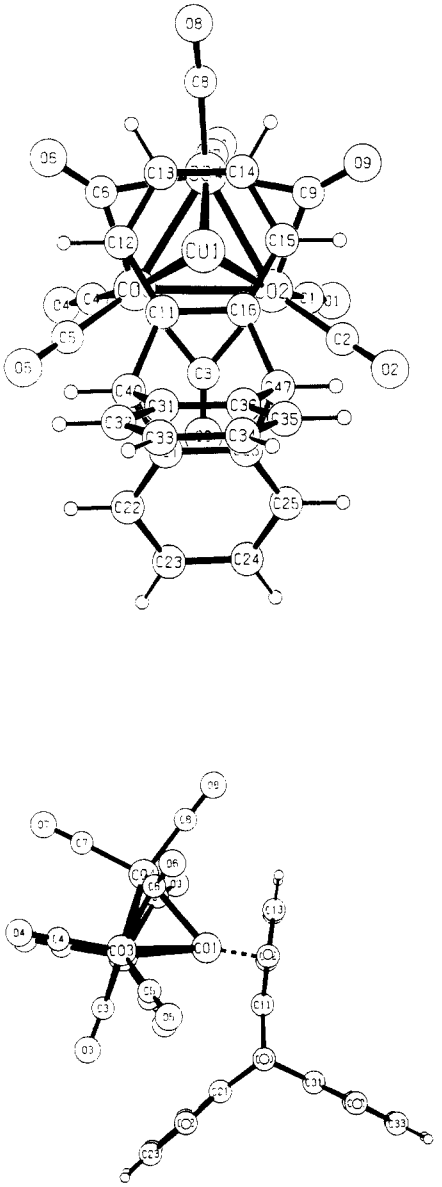

Figure 4. Projections of the structure of nonacarbonyl(η^6-triptycene)tetracobalt (**1**).[2] Top: view down the normal to the least-squares plane of the benzene ring that is coordinated to the apical cobalt atom. Bottom: view down the line connecting the triptycene bridgehead atoms.

above 310 K, 1 ↔ 3 becomes dominant, whereas 2 ↔ 3 predominates below 270 K.

In the case of **1**, rotation about the arene–cobalt axis adds a fourth NMR-detectable process to the three described for **2**. At the slow rotation limit, the molecule most likely adopts a conformation of C_s symmetry, similar to the approximate C_s symmetry of **1** in the crystalline state.[2] In this structure, one each of the three bridging, three axial, and three equatorial carbonyl groups is located in the mirror plane, while the remaining groups are related pairwise by the same plane. Figure 4 (top) shows the three unique carbonyl groups (C3–O3, bridging; C7–O7, axial; C8–O8, equatorial) located on the mirror plane,[25] and the three pairs of symmetry-equivalent (enantiotopic) groups (C6–O6/C9–O9, bridging; C1–O1/C4–O4, axial; C2–O2/C5–O5, equatorial) that are related by that plane. Ac-

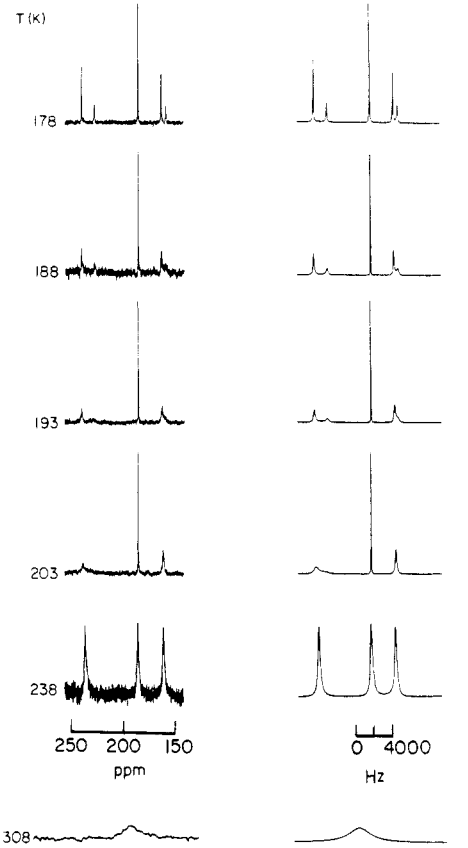

Figure 5. Left: selected variable-temperature ^{13}C NMR spectra (carbonyl region) of nonacarbonyl(η^6-triptycene)tetracobalt (**1**) in CD_2Cl_2. Spectra at 238 K and below were measured at 125.76 MHz. The broad singlet at 308 K (δ 204.2 ($w_{1/2}$ = 85 Hz)) was measured at 22.50 MHz. Right: simulated spectra, using rate constants in Table V.

cording to this analysis, the carbonyl region of the ^{13}C or ^{17}O NMR spectrum of **1** at the slow rotation limit should feature three sets of two signals each, with one signal in each set (the A signal) double the intensity of the other (the B signal). In fact, the 125.76-MHz ^{13}C NMR spectrum of **1** in CD_2Cl_2 at 168 K features two such sets, ν_{1A}/ν_{1B} and ν_{3A}/ν_{3B} (Table III); the third pair ν_{2A}/ν_{2B} appears as a singlet with approximately three times the intensity of the B signals. By analogy to the corresponding signals in **2**, the most downfield signals, ν_{1A}/ν_{1B}, were assigned to the bridging carbonyl carbons. The accidental isochrony of the ν_2 signals provides the clue for the remaining assignments. Inspection of Figure 4 (bottom) shows that two of the three equatorial groups are close to the benzene rings and are therefore expected to experience significant differences in their magnetic environments from the third, whereas all three axial groups are far removed from any shielding effects of the aromatic rings. It is therefore all but certain that the ν_2 signals correspond to the axial and the ν_3 signals to the equatorial carbonyl groups (Table III). The assignments of ν_2 and ν_3 in **2** were made by analogy to these results, and the axial and equatorial carbonyl group signals in the η^6-toluene complex[12,13] may be similarly assigned.

The lowering of symmetry from C_{3v} in **2** to C_s in **1** at the limit of slow rotation and the additional site-exchange process that accompanies rotation about the triptycene–cobalt axis introduces complications in the line-shape analysis of the variable-temperature ^{13}C NMR spectrum of **1** (Figure 5). Thus, there are now 12 distinct processes for carbonyl transpositions, four for each of the three types (Table IV), instead of only three. In addition, rotation

(25) Molecules of **2** in the crystal are located in general positions[2] and are therefore asymmetric. Bilateral (C_s) symmetry, however, is closely approximated (Figure 4, top), and is almost certainly adopted by the free molecule in its ground state.

Table V. Rate Constants for Rotation about the Triptycene–Cobalt Axis (k_r) and for Carbonyl Group Transpositions (k_{ij}) in Nonacarbonyl(η^6-triptycene)tetracobalt (1)

	temperature[b]							
rate const[a]	178	188	193	198	203	208	238	308
$k_r \times 10^{-3}$	0.13	0.35	0.67	1.10	1.90	3.20	35.5	810
k_{13}	0.10	53	63	80	90	100	250	7000
k_{12}	0.10	8.0	12	20	27	41	240	8000
k_{23}	60/40[c]	2.0	4.0	9.0	15	24	600	24350

[a] In s^{-1}. Also see Table I, footnote *a*. [b] In degrees Kelvin. [c] $k_{2A-3A} = 60\ s^{-1}$; $k_{2B-3B} = 40\ s^{-1}$.

Table VI. Activation Parameters for Rotation about the Triptycene–Cobalt Axis (R) and for Carbonyl Group Transpositions (i ↔ j) in Nonacarbonyl(η^6-triptycene)tetracobalt (1)

	process[a]			
parameter	R	1 ↔ 3	1 ↔ 2	2 ↔ 3
E_a[b]	8.2	2.7	6.0	10.1
ln *A*	27.8	11.3	18.3	27.7
ρ[c]	0.9997	0.9979	0.9992	0.9992

[a] See Table II, footnote *a*. [b] In kcal mol^{-1}. [c] Correlation coefficient for the least-squares line through the six k_{ij}'s in the temperature range 188–238 K (Table V).

about the triptycene–cobalt axis exchanges the sites (in and out of the mirror plane) of each of the three types of carbonyl groups and thus gives rise to three more processes, 1A ↔ 1B, 2A ↔ 2B, and 3A ↔ 3B. To determine the best line-shape fit by trial-and-error variation of 15 different rate constants seemed unfeasible, and we therefore simplified the problem by assuming, first, that exchange occurs only between carbonyl groups that are attached to the same cobalt atom, and, second, that the rate constants are not significantly affected by the position of the carbonyl groups relative to the mirror plane. The first assumption eliminates the four processes that are marked with an asterisk in Table IV. The second assumption reduces to four the number of rate constants required to describe the remaining 11 processes: k_r (1A ↔ 1B, 2A ↔ 2B, 3A ↔ 3B), k_{13} (1A ↔ 3A, 1A ↔ 3B, 1B ↔ 3A), k_{12} (1A ↔ 2A, 1A ↔ 2B, 1B ↔ 2A), and k_{23} (2A ↔ 3A, 2B ↔ 3B). The results of this tractable analysis are presented in Table V and in Figure 5.[19]

Arrhenius plots (Figure 6) were constructed by a least-squares fit of the set of six data points for each of the four processes in the range 188–238 K (Table V), corresponding to measurements at high field (125.76 MHz). The poor fit for the carbonyl-exchange processes at the low-temperature limit (178 K) may be due to differences in T_2 for the different carbonyl carbons in **1**,[26] or it may indicate a weakness in our assumption that differences in site symmetry have a negligible effect on the rates of carbonyl exchange,[27] or it may be due to some combination of these or other causes.[28] Arrhenius activation parameters are collected in Table VI.

As in the case of **2**, the relative rates of bridging ↔ axial, bridging ↔ equatorial, and axial ↔ equatorial carbonyl transpositions in **1** are markedly temperature-dependent as a result of entropy factors. The three crossover points fall within the temperature range 210–240 K, and near the middle of this region, at 225 K, $\Delta G^{\ddagger}$ is 10.7, 10.9, and 10.8 kcal mol^{-1} for 1 ↔ 3, 1 ↔ 2, and 2 ↔ 3, respectively. However, now it is 2 ↔ 3 that becomes dominant above 240 K and 1 ↔ 3 that predominates below 210 K—the exact reverse of what is observed for **2** (compare Figures 3 and 6).

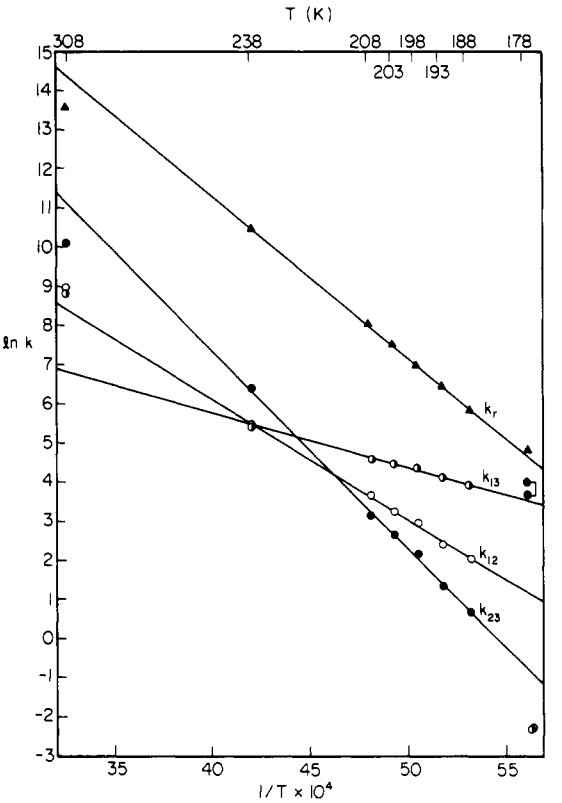

Figure 6. Arrhenius plots for rotation about the triptycene–cobalt axis (k_r) and for the three carbonyl group transpositions (k_{ij}) in nonacarbonyl(η^6-triptycene)tetracobalt (**1**).

Inspection of Figure 6 makes it strikingly evident that rotation about the triptycene–cobalt axis is faster than carbonyl scrambling over the whole temperature range. The free energy of activation (8.2 kcal mol^{-1}) is on the high side of similar arene–metal rotation barriers, as is to be expected from the bulkiness of the hydrocarbon.[29] Extrapolation of the Arrhenius plot for k_r to 308 K, corresponding to a measurement at low field (22.50 MHz),[21] yields a value of $1.85 \times 10^6\ s^{-1}$, as compared to $0.81 \times 10^6\ s^{-1}$ used in the line-shape analysis. Similar extrapolations for k_{12} and k_{23} yield values of 4.4×10^3 and $74 \times 10^3\ s^{-1}$, respectively, as compared to 8×10^3 and $24 \times 10^3\ s^{-1}$ used in the line-shape analysis. In all three cases, the extrapolation yields values for the respective rate constants that

(26) The program DNMR3[17] does not accommodate more than one value of T_2.

(27) Indeed, this assumption, which is the unavoidable price that must be paid in order to reduce the line-shape analysis to manageable proportions, probably breaks down in the neighborhood of the slow-exchange limit. Thus, the best fit for k_{13} at 178 K was obtained by assigning different values for two different processes, 2A ↔ 3A and 2B ↔ 3B (Table V, Figure 6).

(28) Neglect of ^{59}Co quadrupole relaxation on line broadening is not likely to be a significant factor in the observed discrepancy.[23]

(29) $\Delta G^{\ddagger}$ values of 8.4 and 8.5 kcal mol^{-1} were obtained from the coalescence of 3A and 3B at 193 K and of 1A and 1B at 203 K, respectively, by using the Gutowsky–Holm approximation. From the activation parameters for rotation in Table VI, $\Delta G^{\ddagger}$ values of 8.6 and 8.7 are calculated for 193 and 203 K, respectively. The agreement between the two independent sets of calculations lends confidence in our conclusions.

differ by no more than a factor of 2 or 3 from the values used in the line-shape analysis. By contrast, the value of 0.9×10^3 s^{-1} obtained for k_{13} by extrapolation to 308 K differs by a factor of almost 8 from the value of 7×10^3 s^{-1} used in the line-shape analysis. This significant discrepancy in k_{13} values is similar in direction and magnitude to the discrepancy in k_{13} values found for **2** and may, as in the case of **2**, conceivably be due to a change in mechanism at higher temperatures or to the difficulty of obtaining a unique solution.

Experimental Section

Infrared spectra were recorded on a FTS-20C Digilab FT-IR spectrometer. ^1H NMR spectra were recorded at 250.13 MHz on a Bruker WM-250 spectrometer. ^{13}C NMR spectra were recorded at 125.76, 62.83, and 22.50 MHz on Bruker WM-500, Bruker WM-250, and JEOL FX-90Q spectrometers, respectively. All chemical shifts are reported in parts per million downfield relative to tetramethylsilane. Mass spectra were measured on an AEI MS-9 high-resolution mass spectrometer, with an ionizing voltage of 70 eV. Hexane, pentane, and benzene were distilled from sodium benzophenone ketyl and purged with argon before reaction. All reactions were carried out in an inert (argon) atmosphere. Solvent methylene-d_2 chloride (minimum isotopic purity 99.8 atom %) was obtained from MSD Isotopes. Other reagents were obtained from Strem Chemicals (dicobalt octacarbonyl), Aldrich (triptycene and mesitylene), and Cambridge Isotope Laboratories (99 atom% ^{13}CO).

Nonacarbonyl(η^6-triptycene)tetracobalt (**1**) was prepared as described previously.[2] All ^{13}C NMR studies were carried out on material enriched in ^{13}CO, which was prepared from isotopically enriched $Co_4(CO)_{12}$.[30] The extent of labeling, normally 35–50%, was estimated on the basis of the known enrichment of starting $Co_4(CO)_{12}$ and was determined by mass spectrometry. The ^{13}C NMR spectrum in CD_2Cl_2 at 168 K featured five singlets in the carbonyl region, described in Table III.

Nonacarbonyl(η^6-mesitylene)tetracobalt (**2**) was prepared from mesitylene and tetracobalt dodecacarbonyl as described by Bor et al.[6a] IR (hexane): 2074, 2029 (vs), 2010, 1997, 1830 cm^{-1} (lit.[6a] 2072.0, 2028.8 (vs), 2009.6, 1996.8, 1829.0 cm^{-1}). ^1H NMR ($CDCl_3$, ambient temperature) δ 5.92 (3 H, aromatic H), 2.50 (9 H, CH_3) (lit.[6b] δ 5.29, 2.05 (C_6D_6) and δ 5.90, 2.48 (CS_2)). Mass spectrum: m/e 608 (M^+), 580 ($M^+ - CO$), 552 ($M^+ - 2CO$), 524 ($M^+ - 3CO$), 496 ($M^+ - 4CO$), 468 ($M^+ - 5CO$), 440 ($M^+ - 6CO$), 412 ($M^+ - 7CO$), 384 ($M^+ - 8CO$), 356 ($M^+ - 9CO$), 297 ($M^+ - 9CO - Co$), 238 ($M^+ - 9CO - 2Co$), 179 ($M^+ - 9CO - 3Co$), 120 (mesitylene$^+$). All ^{13}C NMR studies were carried out on material enriched in ^{13}CO, which was prepared from isotopically enriched $Co_4(CO)_{12}$.[30] The extent of labeling, normally 35–50%, was determined by mass spectrometry. The ^{13}C NMR spectrum in CD_2Cl_2 at 178 K featured three singlets in the carbonyl region at δ 247.23, 197.25, and 172.68.

A mixture of labeled and unlabeled **2** in CD_2Cl_2 was allowed to stand at room temperature for 5 min and then evaporated to dryness. The mass spectrum of the residue was indistinguishable from that of the same mixture prior to solution, demonstrating that under these conditions no intermolecular exchange of carbonyl groups had taken place. Similar results were obtained for $Co_4(CO)_{12}$.

Variable-Temperature NMR Measurements. Variable-temperature ^{13}C NMR spectra of **1** and **2** in CD_2Cl_2 were recorded at 125.76 MHz (**1**), 62.83 MHz (**2**), and 22.50 MHz (**1** and **2**) in 5-mm sample tubes. Temperatures are considered accurate to ±2 °C. Free energies of activation were calculated from the Eyring equation by least-squares fit of rate constants obtained from line-shape analysis using the program DNMR3.[17] Solvent signals were used for the measurement of internal line width parameters. The effective T_2 was calculated from the relationship $w_{1/2} = 1/\pi T_2$, where $w_{1/2}$ is the width at half-height of the solvent signal.

Acknowledgment. We thank the National Science Foundation (Grant CHE-8009670) for support of this work and Peter Demou and the Yale University Instrumentation Center for assistance in obtaining spectra on the Bruker WM-500 NMR spectrometer.

Registry No. 1, 98104-70-2; 2, 41612-48-0; Co, 7440-48-4.

(30) Darensbourg, D. J.; Zalewski, D. J.; Delord, T. *Organometallics*, **1984**, *3*, 1210. Darensbourg, D. J.; Peterson, B. S.; Schmidt, R. E., Jr. *Ibid.* **1982**, *1*, 306. Bor, G.; Sbrignadello, G.; Noack, K. *Helv. Chim. Acta* **1975**, *58*, 815.